Journal of GeoEngineering, Vol. 11, No. 2, pp. 45-57, August 2016
http://dx.doi.org/10.6310/jog.2016.11(2).1

BEHAVIOR OF GEOTEXTILE-REINFORCED CLAY IN CONSOLIDATED-UNDRAINED TESTS: REINTERPRETATION OF POREWATER PRESSURE PARAMETERS

Kuo-Hsin Yang[1*], Minh Duc Nguyen[2], Wubete Mengist Yalew[3], Chia-Nan Liu[4], and Ranjiv Gupta[5]

ABSTRACT

This paper presents a series of consolidated-undrained triaxial compression tests for investigating the shear behavior of geotextile-reinforced clay and generation of excess porewater pressure during undrained loadings. Specimens were prepared at their maximum dry unit weight and optimum moisture content, and the effects of the confining pressures and the number of geotextile layers were investigated. The experimental results revealed that during consolidation, nonwoven geotextile as a permeable material reduced the time of consolidation; however, it induced a higher volume change. During undrained loading, the shear strength and excess porewater pressure of the reinforced clay increased with the number of geotextile layers because of the restraint of the lateral deformation resulting from the mobilized tensile force of reinforcement layers. Both effective and total stress failure envelopes of the reinforced clay shifted upward as the number of reinforcement layers increased and appeared to be parallel to those of the unreinforced clay. Modified porewater pressure parameters, A^* and B^*, for reinforced clay were proposed using the additional confinement approach. The parameters A^* and B^* can be used to quantitatively evaluate the influence of soil and reinforcement on excess porewater pressure generation, respectively. The A^* value is close to Skempton's porewater pressure parameter A for unreinforced soil. The B^* is defined as the ratio of porewater pressure difference to additional confining pressure. The lower B^* value indicates that the reinforcement is more effective in enhancing additional confining pressure than increasing excess porewater pressure. This study demonstrated that the effect of geotextile layers on inducing additional confinement was more marked than that on the generation of excess porewater pressure, resulting in an increase in effective confining pressure and subsequently in the shear strength of reinforced clay.

Key words: Geotextile-reinforced clay, porewater pressure parameter, triaxial test.

1. INTRODUCTION

Backfill materials are one of the major constituents of geosynthetic-reinforced soil (GRS) structures and account for 30% ~ 40% of their cost (Christopher and Stuglis 2005; Raisinghani and Viswanadham 2011). To achieve effective performance of reinforced earth structures, current design guidelines (Elias *et al*. 2001; AASHTO 2002; Berg *et al*. 2009; NCMA 2010) specify using free-draining granular materials as backfill materials and recommend against the use of fine-grained materials (Fig. 1). Compliant soils (Fig. 1) are backfills that comply with the design guideline criteria, whereas marginal soils are those that do not. In addition to the gradation limits, the plasticity index of the backfill is specified (PI ≤ 6 for walls and 20 for slopes). Because marginal backfills typically have low permeability, they are referred to as poorly draining, low-permeability, low-quality, cohesive, and fine-grained backfills.

To reduce the construction cost of GRS structures, transportation cost, and environmental impact associated with the disposal of the excavated soil, locally available marginal soils have been used as alternative backfills. The main concern regarding the use of marginal soils as backfills is the possibility of a buildup of positive-porewater pressure, which may weaken the soil, resulting in a decrease in the soil shear strength and soil-reinforcement interface strength. However, through the accumulated experience and knowledge gained in both the construction and research of GRS structures with marginal backfills (Sridharan *et al*. 1991; Glendinning *et al*. 2005; Chen and Yu 2011; Taechakumthorn and Rowe 2012; Yang *et al*. 2015), these concerns can be appropriately alleviated by adopting suitable construction techniques and drainage systems. Zornberg and Mitchell (1994) and Mitchell and Zornberg (1995) conducted a comprehensive review of experimental studies and case histories for evaluating the marginal soil-reinforcement interaction mechanism. They presented strong experimental evidence that demonstrate the effectiveness of permeable reinforcement in enhancing the performance and stability of reinforced soil structures constructed using marginal backfills.

Manuscript received November 29, 2015; revised February 22, 2016; accepted April 26, 2016.
[1] Associate Professor (corresponding author), Department of Civil and Construction Engineering, National Taiwan University of Science and Technology, Taipei, Taiwan (e-mail: khy@mail.ntust.edu.tw).
[2] Lecturer, Department of Soil Mechanics and Foundations, University of Technology and Education, Ho Chi Minh City, Vietnam.
[3] Lecturer, Faculty of Civil and Water Resources Engineering, Bahir Dar University, P.O. Box 26, Bahir Dar, Ethiopia.
[4] Professor, Department of Civil Engineering, National Chi-Nan University, Nantou, Taiwan.
[5] Project Engineer, Geosyntec Consultants, 11811N Tatum Blvd., Suite P-186, Phoenix, AZ, 85028, USA.

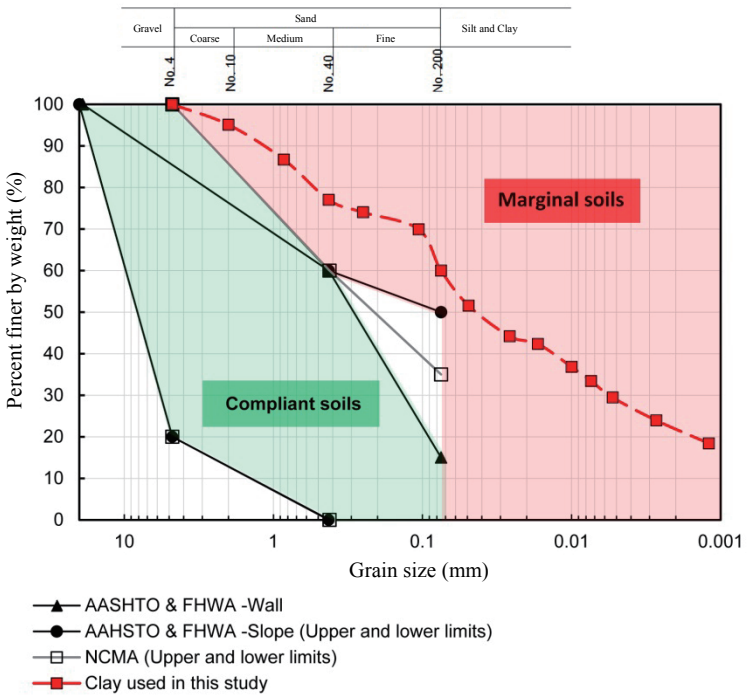

Fig. 1 Grain size distribution of backfill in GRS structures as recommended by design guidelines and tested clay in this study

Triaxial compression tests have been conducted to investigate the responses of reinforced marginal soils under drained and undrained conditions (Ingold 1983; Ingold and Miller 1982, 1983; Fabian and Foure 1986; Fourier and Fabian 1987; Al-Omari *et al*. 1989; Indraratna *et al*. 1991; Unnikrishnan *et al*. 2002; Noorzad and Mirmoradi 2010; Jamei *et al*. 2013; Mirzababaei *et al*. 2013; Yang *et al*. 2015). Ingold and Miller (1982) conducted undrained triaxial tests on kaolin clay reinforced using impermeable aluminum foils and permeable porous plastics and reported that permeable reinforcement exhibited higher performance than impermeable reinforcement did in improving the shear strength of reinforced clay. For clay reinforced with impermeable aluminum foils, the undrained shear strength was substantially less than that of an unreinforced sample, because impermeable reinforcement obstructed the migration of pore pressure inside the specimen in which high excess porewater pressure developed and accumulated at the clay-reinforcement interface, resulting in premature failure along the interface, which in turn caused the failure of the reinforced specimen. They observed that although the permeable reinforcement enhanced the shear strength of reinforced clay, it induced higher porewater pressure during undrained loadings. Ingold and Miller (1982) modified Skempton's porewater pressure parameter A to determine the effect of reinforcement on the generation of porewater pressure and shear strength improvement.

Fabian and Fourie (1986) evaluated the influence of the permeability of the reinforcing material on the undrained shear strength of reinforced clay through unconsolidated-undrained (UU) triaxial tests and found that high-permeable reinforcements increase the undrained shear strength of the reinforced clay by almost 40%, whereas low-permeable reinforcements can decrease the undrained strength by a similar amount. They observed that the permeability of reinforcement influenced water migration and moisture distribution within specimens, resulting in their differential effects on clay-reinforcement interaction.

Al-Omari *et al*. (1989) performed consolidated-undrained (CU) and consolidated-drained (CD) triaxial tests to investigate the response of clay reinforced with geomesh. The results revealed that the failure of overconsolidated geomesh-reinforced clay was due to progressively developed slippage at the clay-geomesh interface. The excess porewater pressure developed in the reinforced clay was higher than that in the unreinforced clay, and this pressure increased with the number of reinforcement layers. Noorzad and Mirmoradi (2010), Mirzababaei *et al*. (2013), and Yang *et al*. (2015) conducted unconfined compression and UU tests on reinforced clay and reported that inclusion of permeable reinforcement into clay can considerably enhance the peak soil shear strength, reduce postpeak strength loss, and change the failure behavior from brittle to ductile. The shear strength of the reinforced specimen was affected by the soil plasticity index, compaction conditions (*i.e.*, moisture content and relative compaction), and number of reinforcement layers.

In the study of reinforced marginal backfill, an important question to answer is what the porewater pressure generation within reinforced structures is during construction and loadings (Fig. 2). The key to this question is to determine the relationship between porewater pressure and the applied loadings. The assessment of porewater pressure generation and its relation to the shear strength improvement of reinforced clay is crucial for analyzing the effectiveness and suitability of applying reinforcement to marginal backfill. Therefore, in this study, a series of CU triaxial tests were performed on reinforced clay with nonwoven geotextile. The objective of these tests were threefold: (1) to investigate the shear response of clay reinforced with different number of reinforcement layers under undrained loadings; (2) to investigate the generation of excess porewater pressure and its relation to the shear strength of reinforced clay; and (3) propose a modified porewater pressure parameter for assessing the effect of reinforcement on porewater pressure generation and soil shear improvement. Based on the concept of reinforcement-induced additional confinement, this paper explains the counterintuitive observation reported in the literature that permeable reinforcement enhances the shear strength of reinforced clay but induces higher porewater pressure under undrained conditions. The results and discussion in this paper are useful for more clearly understanding the shear behavior and porewater pressure generation of reinforced clay.

2. EXPERIMENTAL PROGRAM

Twelve CU triaxial compression tests were performed at different effective consolidation pressures ($\sigma'_{3,con}$ = 50, 100, and 200 kPa) and various numbers of geotextile layers (unreinforced and 1 ~ 3 layers). The undrained test conditions were selected to simulate the behavior of cohesive soils subject to undrained loadings (relative to the time required for the dissipation of porewater pressure of cohesive soils) after construction. Several experimental tests performed to determine the index and engineering properties of the tested clay and nonwoven geotextile are described in this section.

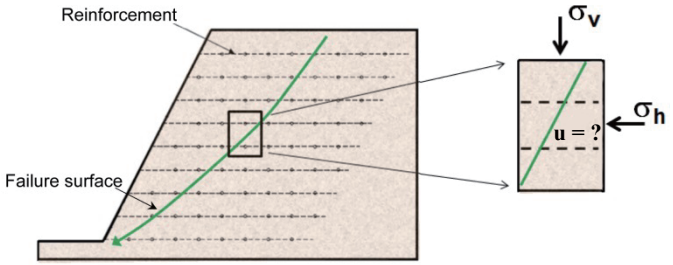

Fig. 2 Illustration of porewater pressure generation in reinforced structures with marginal backfill

2.1 Test Materials

2.1.1 Clay

Clay soil obtained from Maokong area, southeast mountain region of Taipei, Taiwan, was used in this study. Figure 1 shows the grain size distribution of tested soil based on ASTM D422. Table 1 summarizes properties of the clay. This clay is classified as low-plasticity clay (CL) by the Unified Soil Classification System with specific gravity, G_s = 2.72, liquid limit, LL = 42, plastic limit, PL = 21, and plasticity index, PI = 21. The optimum moisture content and maximum dry unit weight determined from standard proctor compaction (ASTM D698) are ω_{opt} = 19.2% and $\gamma_{d,\max}$ = 15.1 kN/m^3, respectively (Fig. 3). The saturated hydraulic conductivity estimated using Terzaghi's 1-D consolidation theory is k_{sat} = 1.3 × 10^{-10} m/s. The total and effective shear strength parameters for clay were c = 57.6 kPa; ϕ = 15.3° and c' = 10.7 kPa; ϕ' = 29.2°, respectively. The determination of shear strength parameters obtained from the CU tests is discussed later.

2.1.2 Geotextile

A commercially available needle-punched PET nonwoven geotextile was used. Table 2 summarizes properties of the tested nonwoven geotextile. The load-elongation behavior of the reinforcement was obtained by wide-width tensile tests (ASTM D4595) in the longitudinal and transverse directions (Fig. 4). The tensile test results indicate that the geotextile is an anisotropic tensile material; the tensile strength and stiffness of the geotextile in the longitudinal direction (*i.e.*, the stronger and stiffer direction) were larger than those in the transverse direction (*i.e.*, the weaker and softer direction). Based on permittivity test results (ASTM D4491), this geotextile has a permittivity ψ = 1.96 s^{-1} and the corresponding cross-plane permeability of k = 3.5 × 10^{-3} m/s. The permeability of the nonwoven geotextile is several orders of magnitude higher than the permeability of the clay used in this study; therefore, the nonwoven geotextile could be considered a permeable material.

2.2 Specimen Preparation

A natural clay sample brought from a local site in the form of wet bulk was placed in an oven for a minimum of 24 h and then crushed and ground into dry powder in a mortar. Accurately measured quantities of dry powder soil and water corresponding to optimum moisture content were mixed together, placed in a plastic bag within a temperature-controlled chamber and sealed for a minimum of 2 days to ensure a uniform distribution of moisture within the soil mass. The moisture content was verified to ensure that the variation of moisture content was less than 1%.

Table 1 Properties of the tested clay

Properties	Value
Unified soil classification system	CL
Fine content (%)	67.6
Specific gravity, G_s	2.70
Liquid Limit, LL (%)	42
Plastic Limit, PL (%)	21
Plasticity Index, PI (%)	21
Optimum moisture content, ω_{opt} (%)	19.2
Maximum dry density, $\gamma_{d,\max}$ (kN/m^3)	15.1
Total cohesion, c (kPa)	59.3
Total friction angle, ϕ (°)	15.6
Effective cohesion, c' (kPa)	11
Effective friction angle, ϕ' (°)	29.7
Saturated hydraulic conductivity, k_{sat} (m/s)	1.3 × 10^{-10}

Table 2 Properties of the nonwoven geotextile

Properties	Value
Mass (g/m^2)	200
Thickness, t (mm)	1.78
Apparent opening size, AOS (mm)	0.11
Permittivity, ψ (s^{-1})	1.96
Cross-plane permeability, k (m/s)	3.5 × 10^{-3}
Ultimate tensile strength, T_{ult} (kN/m)	9.28 and 7.08
Failure strain (%)	84.1 and 117.8
Secant stiffness at peak value (kN/m)	11.03 and 6.01

Note: The thickness was measured according to ASTM D5199. The first and second values of tensile properties correspond to the test results in longitudinal and transverse directions, respectively.

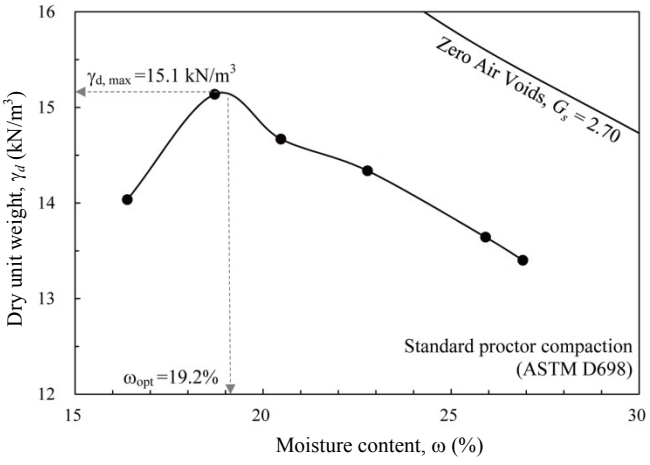

Fig. 3 Standard compaction curve of the tested clay

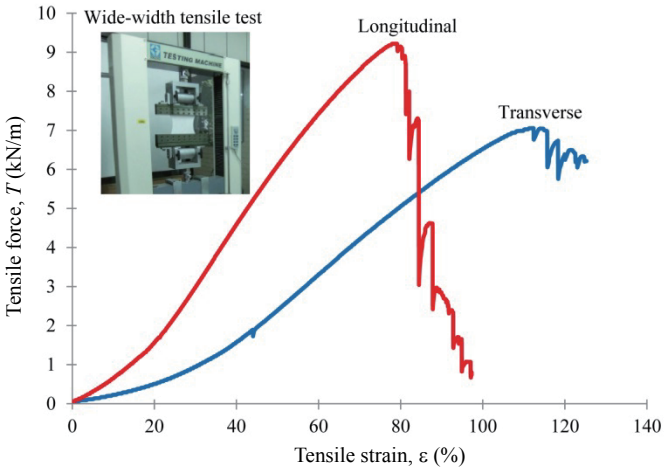

Fig. 4 Tensile load-elongation response of nonwoven geotextile

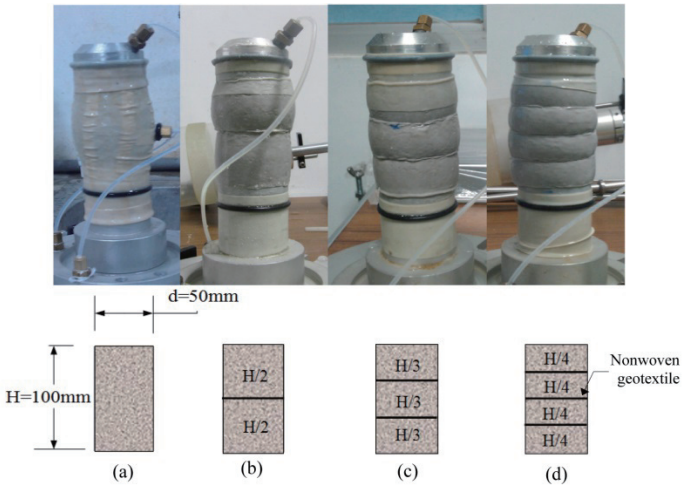

Fig. 5 Reinforcement arrangement and failure pattern of clay specimens for CU triaxial tests: (a) Unreinforced; (b) 1 layer; (c) 2 layers; (d) 3 layers

The test specimens with a diameter of 50 mm and a height of 100 mm were prepared. For the unreinforced specimens, the clay was compacted in five layers. Each layer was initially lightly tamped to avoid any honeycombs within the samples. The samples were then statically compressed to the required thickness by a static hydraulic jack.

For the reinforced clay specimens, the split mold was filled with clay in several layers, depending on the arrangement of the geotextile layers (Fig. 5). After each clay layer was compacted and leveled, the clay surface was scarified prior to adding the overlying geotextile layer and the next soil layer for developing favorable interface bonding with the overlying material. The reinforcement was then placed horizontally, and the amount of soil for the next layers was poured and compacted. This procedure was repeated until specimen preparation was completed.

2.3 Test Procedure

CU triaxial tests were conducted according to the ASTM D4767. The prepared specimen was placed in a triaxial cell and saturated by allowing de-aired water to flow through the system. A back pressure was applied to facilitate the saturation of the soil specimen in which the difference between the back and chamber pressures was maintained lower than 25 kPa. Skempton's porewater pressure coefficient B was monitored during saturation until its value exceeded 0.95. Three effective consolidation pressures ($\sigma'_{3,con}$ = 50, 100, and 200 kPa) were applied in the test program. The volume change in specimens with time was recorded to calculate the time for 50% of the primary consolidation t_{50}. After the consolidation phase was complete, the specimens were loaded axially under an undrained condition at a strain rate $\dot{\varepsilon}$, determined as follows:

$$\dot{\varepsilon} = \frac{\varepsilon_f}{10 \times t_{50}} \quad (1)$$

where ε_f is the strain at failure. The calculated average strain rates were 0.035 ~ 0.060 %/min for specimens with various reinforcement arrangements (Table 3). These applied strain rates can produce approximate equalization of porewater pressures through the specimen, thus permitting the accurate measurement of porewater pressure and determination of effective stress envelope. All tests were completed when the axial strain of the reinforced soil reached 20%. The repeatability and consistency of the test results were carefully examined by conducting a few tests on the reinforced clay under the same conditions.

Table 3 Time for 50% of volume change under consolidation process

$\sigma'_{3,con}$ (kPa)	t_{50} (sec)			
	Unreinforced	1 layer	2 layers	3 layers
50	1802	1498	1254	1012
100	1602	1449	1210	973
200	1452	1348	1156	925
Average strain rate (%/min)	0.035	0.040	0.050	0.060

3. RESULTS AND DISCUSSION

The experimental results from the consolidation and undrained loading phases are presented and discussed here.

3.1 Volume Change with Time in the Consolidation Phase

The variations in volume change ΔV with time of the unreinforced and reinforced specimens in the consolidation phase were recorded (Fig. 6). The volume for all the specimens decreased (positive value of ΔV in Fig. 6 indicates compression) as the porewater dissipated until equilibrium was reached (*i.e.*, complete consolidation). The consolidation results indicated that the nonwoven geotextile facilitates porewater dissipation by reducing the vertical drainage path within the specimen. The time required time to reach t_{50} decreases as the number of reinforcement layers or $\sigma'_{3,con}$ increases. The permeable reinforcement is more influential than $\sigma'_{3,con}$ is on t_{50} reduction. As shown in Table 3, when the number of reinforcement layers was doubled, the

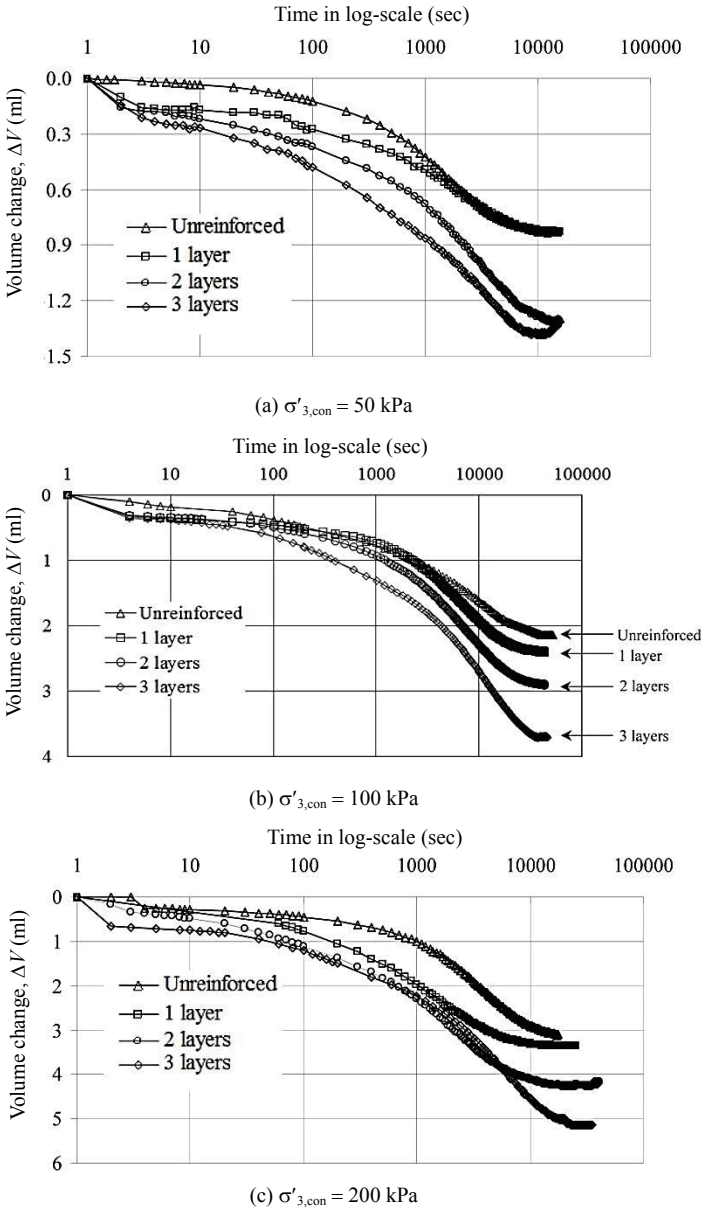

Fig. 6 Volume change vs. time during consolidation for specimens with various numbers of reinforcement layers and under different $\sigma'_{3,con}$

time reduction to reach t_{50} was approximately 110 ~ 300 s, substantially higher than that (50 ~ 100 s) after doubling the $\sigma'_{3,con}$ values. Notably, filter paper strips were used for unreinforced specimens to facilitate the porewater pressure dissipation during consolidation but no filter paper was attached to the reinforced specimens because: 1. the permeable geotextile can also drain water; 2. the bonding between clay and reinforcement layers may be detached when introducing the filter paper strips to the reinforced specimens by removing the specimens out of split mold. Even though there is a difference in the use of filter papers, the test results (Fig 6 and Table 3) indicated that the permeable geotextile was more effective in accelerating consolidation than the filter paper.

Moreover, a higher volume reduction occurred in the specimens reinforced with more reinforcement layers. Because of the high compressibility of nonwoven geotextile, the consolidation pressure easily compresses the nonwoven geotextile layer and squeezes out more water, inducing higher volume change in the reinforced specimens. The more the reinforcement layers of the reinforced specimens, the higher the volume reduction. In summary, the use of permeable geotextile reduces the consolidation time (more effectively than applying higher consolidated pressure does) but induces more deformation during consolidation phase.

The measured volume change in the unreinforced clay during the consolidation phase was used for estimating the preconsolidation pressure σ'_c caused by the applied compaction energy during specimen preparation. The initial void ratio $e_0 = 0.779$ in the e-log p' curve (Fig. 7) was calculated using the volume of solid $V_s = 110.36$ ml and volume of void $V_v = 85.99$ ml. Subsequently, the measured volume change at the completion of consolidation was applied to estimate the void ratio change corresponding to each consolidation pressure. By following the graphical procedure suggested by Casagrande (1936), the preconsolidation pressure was determined as $\sigma'_c = 110$ kPa (Fig. 7). Therefore, the specimens under $\sigma'_{3,con} = 50$ and 100 kPa were lightly overconsolidated (OCR = 2.2 and 1.1, respectively) and those under $\sigma'_{3,con} = 200$ kPa were normally consolidated.

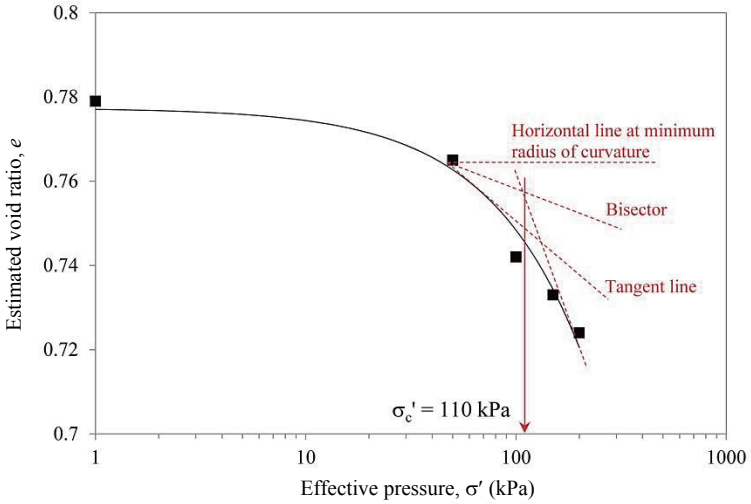

Fig. 7 Estimate of preconsolidation pressure in e-log p′ curve

3.2 Shear-Strain Behavior

Figures 8 ~ 10 illustrate the stress-strain and excess porewater pressure responses of the unreinforced and reinforced clay specimens for various $\sigma'_{3,con}$. Because all specimens exhibited hardening, no definite peak was noticed on the stress-strain curve. Therefore, the strain level of $\varepsilon_1 = 15\%$ was considered the failure strain, as suggested in ASTM D4767.

As shown in Figs. 8 ~ 10, at a given confining pressure, the reinforced clay specimens reached higher peak shear strengths compared with the unreinforced specimens. The peak shear strength increased as the number of geotextile layers and confining pressure increased. The presented stress-strain curves provide strong evidence that including permeable reinforcements can effectively improve the shear strength of clay under undrained loadings. The similar observation was reported by Ingold and Miller (1982), Fourie and Fabian (1986), Al-Omari *et al.* (1989),

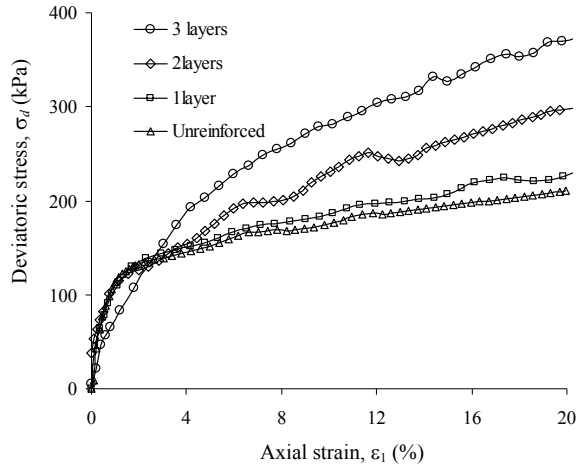

(a) Stress-strain response

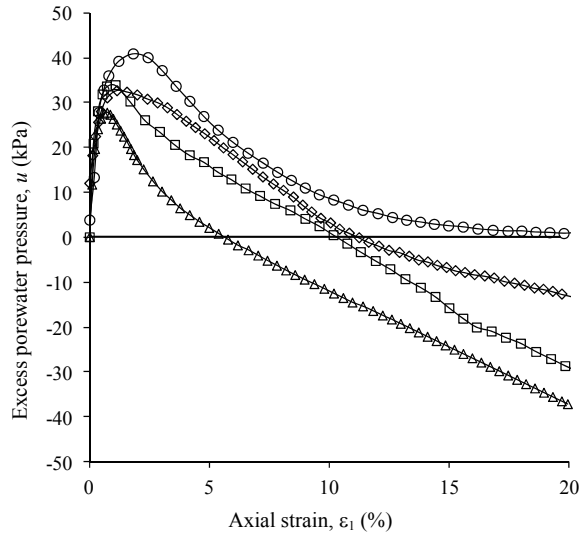

(b) Excess porewater pressure-strain response

Fig. 8 Stress-strain and excess porewater pressure responses of clay specimens at $\sigma'_{3,con}$ = 50 kPa

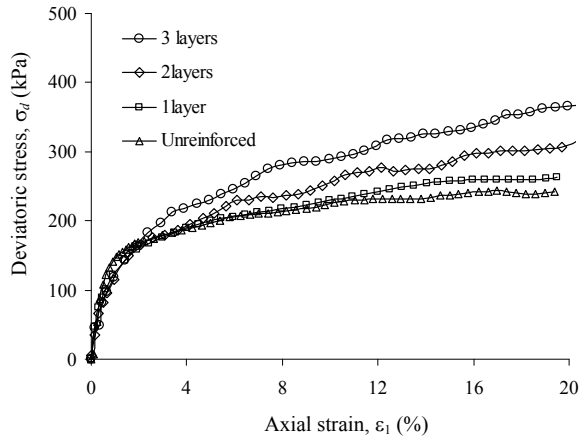

(a) Stress-strain response

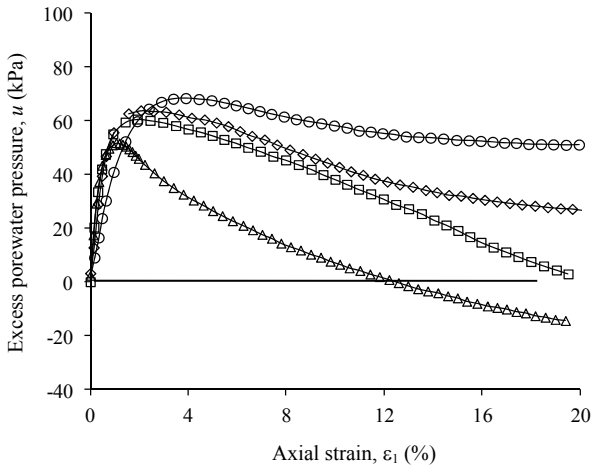

(b) Excess porewater pressure-strain response

Fig. 9 Stress-strain and excess porewater pressure responses of clay specimens at $\sigma'_{3,con}$ = 100 kPa

Athanasopoulos (1993), and Unnikrishnan *et al*. (2002). The reinforcing mechanism is attributed to the mobilized tensile force in geotextile layers through soil-reinforcement interaction. By experimentally inspecting the mobilized tensile strain of reinforcement, Nguyen *et al*. (2013) and Yang *et al*. (2015) demonstrated a direct and linear relationship between the mobilized reinforcement tensile strain/load and shear strength improvement of reinforced soil.

A minor difference was observed between the σ_d values of the unreinforced and reinforced clay specimens at low strain levels (approximately for $\varepsilon_1 < 3\%$), indicating that the geotextile reinforcement requires sufficient deformation to mobilize its tensile force, which then contributes to the overall shear strength improvement of the reinforced soil. The effects of reinforcement were activated (*i.e.*, the mobilized shear strength of the reinforced soil exceeded that of the unreinforced soil) under an axial strain of approximately up to 3%. This finding is consistent with the observations from the test results of reinforced sand (Nguyen *et al*. 2013) and reinforced clay (Fourie and Fabian 1987; Al-Omari *et al*. 1989; Unnikrishnan *et al*. 2002; Noorad and Mirmoradi 2010).

3.3 Excess Porewater Pressure

Figures 8 ~ 10 illustrate the excess porewater pressure responses of the unreinforced and reinforced clay for various $\sigma'_{3,con}$. For all specimens, the porewater pressure initially increased, peaked at approximately $\varepsilon_1 = 1 \sim 3\%$, and then decreased gradually. At a low axial strain level, the compression of clay specimens subject to loadings increased the porewater pressure. After reaching a certain threshold of axial deformation ($\varepsilon_1 = 1 \sim 3\%$), the specimens began to dilate, inducing the decrease in porewater pressure. For the specimens under $\sigma'_{3,con}$ = 50 and 100 kPa (lightly overconsolidated specimens as discussed in Section 3.1), a negative porewater pressure was generated at a high strain level.

The influence of reinforcement on the porewater pressure depends on the strain level. To justify this statement, the values of porewater pressure u and porewater pressure difference Δu_r between the reinforced and unreinforced specimens at ε_1 = 2% (*i.e.*, the average axial strain for the peak porewater pressure) and 15% (*i.e.*, at limit state) were calculated and are listed in Table 4. At ε_1 = 2%, a clear increasing or decreasing trend of u and Δu_r with an increase in the number of reinforcement layers is not

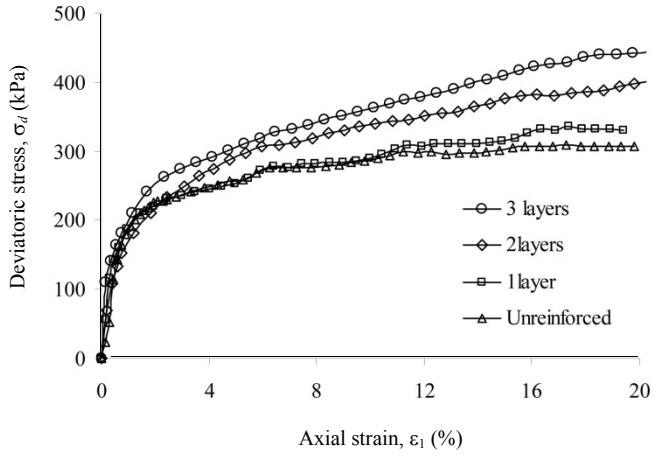

(a) Stress-strain response

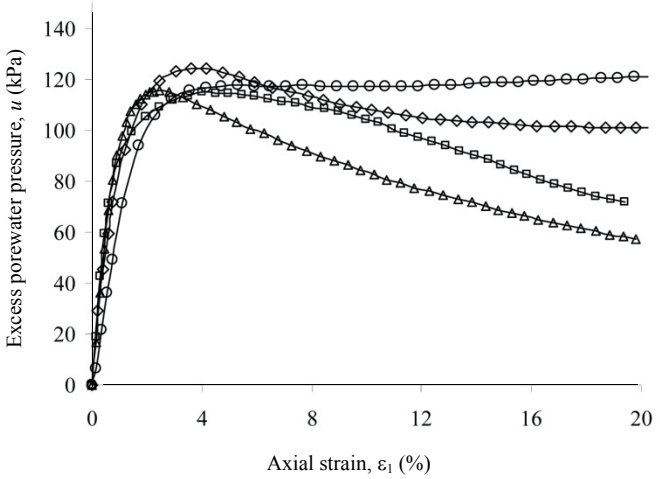

(b) Excess porewater pressure-strain response

Fig. 10 Stress-strain and excess porewater pressure responses of clay specimens at $\sigma'_{3,con}$ = 200 kPa

observed. By contrast, at ε_1 = 15%, u and Δu_r exhibit a consistent increasing trend with an increase in the number of reinforcement layers. In other words, the excess porewater pressure developed in the reinforced clay at failure was higher than that in the unreinforced clay, and it increased with the number of reinforcement layers.

As discussed previously, the effects of reinforcement were activated under an axial strain of approximately 3%. Therefore, at ε_1 = 2%, the required deformation was insufficient to activate the effect of reinforcement; the generation of porewater pressure appears to be independent of the presence of reinforcement layers. At ε_1 = 15%, the effect of reinforcement has been already activated at such a considerably high strain level. The mobilized tensile force restrained the lateral deformation of clay and thus prevented the clay from dilating. This effect became more marked as the number of reinforcement layers increased. Therefore, a clear increasing trend of u and Δu_r with an increase in the reinforcement layers was observed (Table 4). This observation was supported by the experimental results reported by Ingold (1983), Ingold and Miller (1982), and Al-Omari *et al*. (1989).

Table 4 Generation of excess porewater pressure of unreinforced and reinforced clay at ε_1 = 2% and 15% under different $\sigma'_{3,con}$ values

	ε_1 = 2%		ε_1 = 15%	
Cases	u (kPa)	Δu_r (kPa)	u (kPa)	Δu_r (kPa)
$\sigma'_{3,con}$ = 50 kPa				
Unreinforced	17.2	0	–24.4	0
1 layer	28.8	11.6	–15.8	8.6
2 layers	31.7	14.5	–6.7	17.7
3 layers	40.9	23.7	2.5	26.9
$\sigma'_{3,con}$ = 100 kPa				
Unreinforced	46.0	0	–6.0	0
1 layer	60.6	14.7	19.6	25.6
2 layers	63.4	17.5	32.1	38.1
3 layers	59.8	13.8	52.8	58.8
$\sigma'_{3,con}$ = 200 kPa				
Unreinforced	113.9	0	68.2	0
1 layer	105.4	–8.5	81.0	12.8
2 layers	110.1	–3.8	102.5	34.3
3 layers	98.5	–15.4	118.7	50.5

Both the shear strength and excess porewater pressure of the reinforced clay increased as the number of reinforcement layers increased. Unexpectedly, the higher shear strength improvement was associated with higher porewater pressure under undrained loadings. These results appear to be the reverse of what would be expected. As a result, the inclusion of reinforcement layers must have caused an increase in the total confining pressure, $\Delta\sigma_3$, which is higher than the porewater pressure difference at failure Δu_r by an amount of effective confining pressure $\Delta\sigma'_3$. Subsequently, the increase in $\Delta\sigma'_3$ caused the shear strength improvement of the reinforced clay. This observation is explained in Section 4. A modified porewater pressure parameter, based on the concept of additional confinement induced by geotextile layers, was proposed to evaluate the effect of reinforcement on porewater pressure generation and its relation with soil shear improvement.

3.4 Failure Pattern

Figure 5 shows typical images of the unreinforced and reinforced specimens after the tests. The unreinforced specimen failed after bulging at its middle. The reinforced clay specimens (Fig. 5(b) ~ 5(d)) failed when bulging occurred between two adjacent reinforcement layers. The inclusion of reinforcement restrained the lateral displacement of soil near the reinforced area and consequently, larger soil displacement occurred between two adjacent reinforcement layers. As the number of geotextile layers was increased (*i.e.*, the shorter vertical reinforcement space), the deformation became comparatively uniform (less bulging). The uniform deformation of a specimen suggested that the mobilized

stresses were redistributed evenly within the soil, thus enhanced the shear strength of the reinforced soil. A similar behavior of the reinforced specimens was reported by Nguyen *et al*. (2013), Haeri *et al*. (2000), and Khedkar and Mandal (2009) for reinforced sand and Fourie and Fabian (1986) for reinforced clay. Posttest examinations by retrieving geotextile from the dismantled specimens revealed that geotextile was intact (no rupture) at an axial strain of 20% at test completion.

3.5 Failure Envelope and Stress Path

Figure 11 exhibits the total and effective stress failure envelopes of the unreinforced and reinforced clay in the p-q diagram (MIT stress path approach). As the number of reinforcement layers increased, the failure envelopes of the reinforced specimens shifted upward, and both effective and total stress envelopes appeared to be parallel to those of the unreinforced clay. The cohesion intercept increased, whereas the angle of internal friction was not altered. Figure 11 also presents the effective and total stress shear strength parameters. The results for failure envelopes in this study are consistent with those for triaxial tests by Gray and Al-Refeai (1986) and Haeri *et al*. (2000) for reinforced sand and Noorzad and Mirmoradi (2010) and Al-Omari *et al*. (1989) for reinforced clay under undrained conditions.

The contribution of reinforcement on shear strength improvement can be explained using the concept of apparent cohesion as adding an apparent cohesion to the unreinforced soil (Schlosser and Long 1974; Hausmann 1976; Bathurst and Karpurapu 1993) or using the concept of additional confinement as an increase in the effective confining pressure (Ingold and Miller 1983; Chandrasekaran *et al*. 1989; Wu and Hong 2008). In the apparent cohesion concept, the contribution of nonwoven geotextile to shear strength improvement can be attributed to an increase in the apparent cohesion of the reinforced clay (as the parallel failure envelopes shown in Fig. 11). For the additional confinement concept, reinforced soil at the limit state is assumed to have the same effective principal stress relationship (*i.e.*, the same failure envelope) as unreinforced soil does:

$$\sigma_1' = (\sigma_3' + \sigma_{3add}') \tan^2\left(45 + \frac{\phi'}{2}\right) + 2c' \tan\left(45 + \frac{\phi'}{2}\right) \qquad (2)$$

where σ'_1 is the effective axial stress of the reinforced soil at failure, σ'_3 and σ'_{3add} are the effective confining pressure of the unreinforced soil at failure and effective additional confining pressure induced by reinforcement, and ϕ' and c' are the effective friction angle and cohesion of the unreinforced soil.

Therefore, σ'_{3add} can be estimated as

$$\sigma_{3add}' = \sigma_1' \tan^2\left(45 - \frac{\phi'}{2}\right) - 2c' \tan\left(45 - \frac{\phi'}{2}\right) - \sigma_3' \qquad (3\text{-}1)$$

or

$$\sigma_{3add}' = \sigma_1' K_a - 2c'\sqrt{K_a} - \sigma_3' \qquad (3\text{-}2)$$

where K_a is the active earth pressure coefficient. The σ'_{3add} in Eq. (3) is the accumulated additional confining pressure at failure. To trace the stress path, the development of effective additional confining pressure was assumed to be proportional to the mobilization of the soil shear strength. In addition, an increase in effective

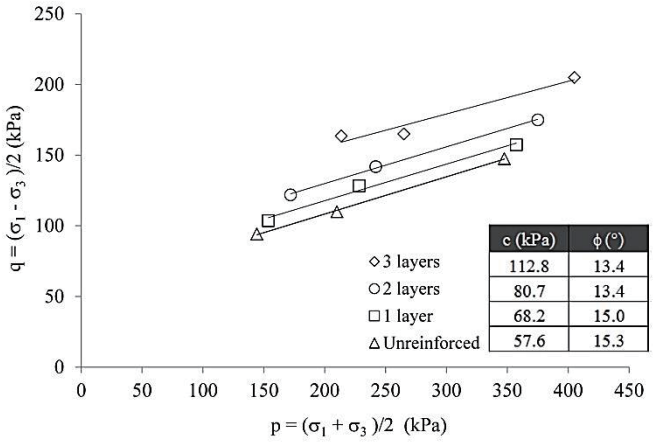

(a) Total stress envelope

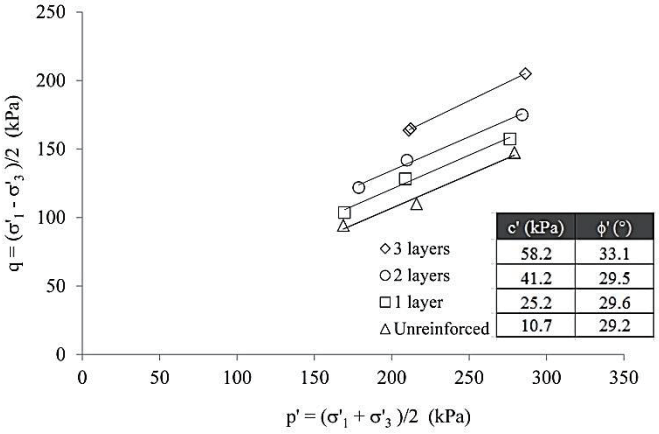

(b) Effective stress envelope

Fig. 11 Failure envelope: (a) total stress envelope; (b) effective stress envelope

additional confining pressure σ'_{3add} was associated with an enhanced porewater pressure Δu_r relative to the porewater pressure of the unreinforced soil. Δu_r is the porewater pressure difference between the reinforced and unreinforced soil and can be perceived as the porewater pressure induced exclusively by the effect of reinforcement. The total additional confining pressure σ_{3add} at the soil limit state can be calculated as follows:

$$\sigma_{3add} = \sigma_{3add}' + \Delta u_r \qquad (4)$$

Figure 12 illustrates the total stress paths (TSPs) in the principal space for the unreinforced and reinforced clay with three nonwoven geotextile layers under $\sigma'_{3,con}$ = 50 and 200 kPa. As shown in Fig. 12, all the stress paths initiate at the isotropic consolidation line. The TSPs of the unreinforced clay rose straightly up and reached the unreinforced failure envelope. The TSPs of the reinforced clay also increased and reached the reinforced failure envelope at a σ_1 higher than that of the unreinforced clay. The difference between the unreinforced and reinforced failure envelopes can be attributed to the apparent cohesion induced by the inclusion of the reinforcement layers.

When applying the additional confinement concept to reinforced clay, the total confining pressure increases when considering σ_{3add} derived from Eq. (4). The estimated TPS of the

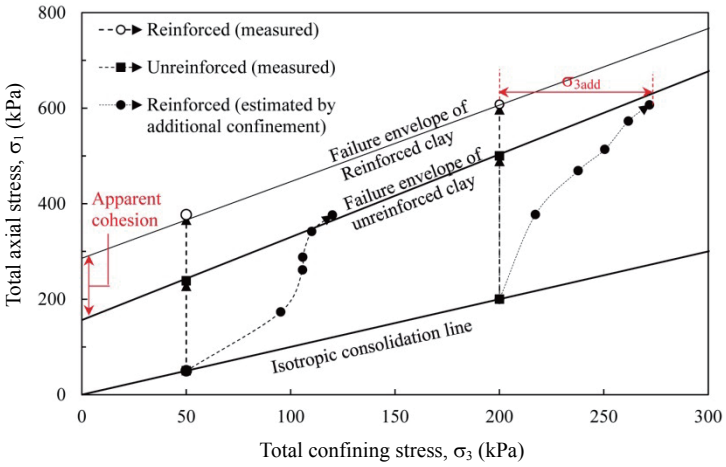

Fig. 12 Total stress path of unreinforced and reinforced clay and TPS estimated by additional confinement approach

reinforced clay gradually turned right because of the effect of σ_{3add}. The TPSs of the unreinforced and reinforced specimens (based on additional confinement) approached the same failure envelope (*i.e.*, the failure envelope of the unreinforced soil), and the only difference is that the reinforced specimen reached a higher σ_1 value than the unreinforced specimen did. Notably, the TSPs of the reinforced clay estimated by the additional confinement concept reached the same σ_1 values as the measured TSPs of the reinforced clay (*i.e.*, apparent cohesion concept). The key to understand this discussion is that one can consider the unreinforced and reinforced soil as the same soil under different confining pressures (because of the effect of reinforcement). When subject to axial loadings, their stress paths converge onto the same stress envelope. The soil under a high confining pressure (in the case of the reinforced specimen interpreted through additional confinement concept) reaches a higher shear strength compared with the soil under a low confining pressure (in the case of the unreinforced specimen). As a result, as demonstrated in Fig. 12, the effect of reinforcement layers can be modeled in terms of additional confinement.

4. POREWATER PRESSURE PARAMETER

This section first reviews Skempton's porewater pressure parameters and the porewater pressure parameters proposed by Ingold and Miller (1982). The modified porewater pressure parameters of the reinforced clay are then introduced. Subsequently, the porewater pressure parameters calculated through different methods are compared to examine their effectiveness and suitability for assessing the influence of reinforcement on excess porewater pressure generation during undrained loadings.

4.1 Definition of Porewater Pressure Parameter in the Literature

Porewater pressure parameters were first proposed by Skempton (1954) to express the changes in pore pressure Δu, which occur under changes in the total stresses, by using the following equation:

$$\Delta u = B\left[\Delta\sigma_3 + A(\Delta\sigma_1 - \Delta\sigma_3)\right] \tag{5}$$

where A and B are the conventional Skempton's porewater pressure parameters, and $\Delta\sigma_1$ and $\Delta\sigma_3$ are changes in the major and minor principal stresses, respectively. Under triaxial test conditions, the pore pressure parameter B describes the relation between the applied confining pressure and the corresponding porewater pressure change during the consolidation phase, and parameter A defines the relation between the applied deviatoric stress and the corresponding porewater pressure change during the undrained loading phase. In a CU triaxial test, for saturated, normally consolidated, and lightly overconsolidated soil, the parameter $B = 1.0$ can be assumed; then, parameter A (or $\bar{A}$) at a given stress level can be expressed as:

$$A = \frac{\Delta u}{\Delta\sigma_1} = \frac{\Delta u}{\Delta\sigma_d} \tag{6}$$

where $\Delta\sigma_d$ denotes changes in the deviatoric stress at a given stress level, which equals the changes in the major principal stress. Parameter A at the soil limit state is represented as

$$A = \frac{u}{\sigma_d} \tag{7}$$

where u and σ_d are the porewater pressure generation and deviatoric stress at failure, respectively.

Ingold and Miller (1982) modified the porewater pressure parameter A' to account for the porewater pressure generation of reinforced specimens under undrained loadings. Ingold and Miller's approach was deduced from Skempton's general porewater equation (Eq. (5)) and used additional confinement (Eqs. (3) and (4)). Combining Eqs. (4) and (5),

$$u = B'\left[\sigma_{3add} + A'(\sigma_d - \sigma_{3add})\right] \tag{8}$$

Assuming $B' = 1$ for saturated reinforced specimens, Ingold and Miller's porewater pressure parameter A' for the reinforced clay at the soil limit state is evaluated as

$$A' = \frac{u - \sigma_{3add}}{\sigma_d - \sigma_{3add}} \tag{9}$$

4.2 Modified Porewater Pressure Parameters

When using Ingold and Miller's porewater pressure parameter A' for the reinforced clay, two problems are identified:

1. The assumption of $B' = 1$ for the reinforced soil is invalid. Figure 13 illustrates the relationship of the total additional confining pressure σ_{3add} with the porewater pressure difference Δu_r induced by reinforcement. All data points lie above the 1:1 ($B' = 1$) line, suggesting that the effect of reinforcement on the total additional confining pressure is more marked than on the excess porewater pressure generation (*i.e.*, $\sigma_{3add} > \Delta u_r$). The data points move farther from the 1:1 line as the number of reinforcement layers increases.

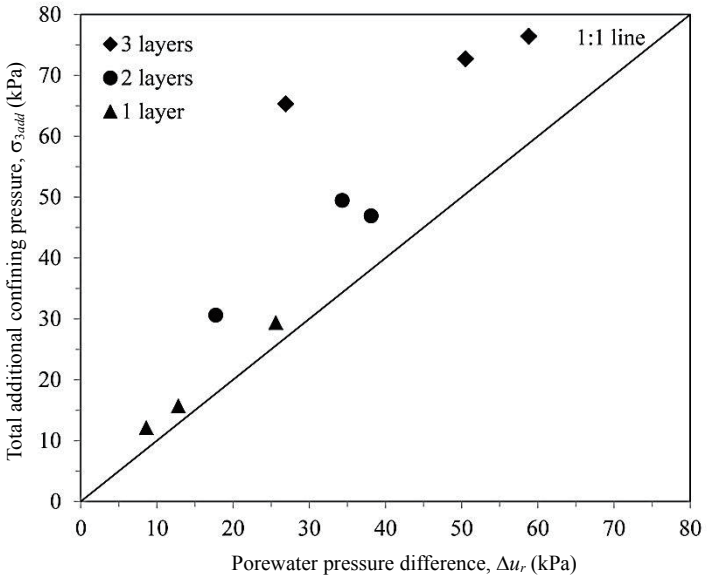

Fig. 13 Comparison between porewater pressure difference Δu_r and total additional confining pressure σ_{3add} for reinforced clay under undrained loadings

2. The effects of soil, stress history (OCR), and reinforcement on excess porewater pressure generation are combined in Ingold and Miller's porewater pressure parameter A'. Therefore, distinguishing the influence of soil and reinforcement separately becomes difficult, making it impossible to assess the effect of reinforcement on porewater pressure generation.

Accordingly, this study proposed two modified porewater pressure parameters, A^* and B^*, for the reinforced clay to more efficiently quantify the influence of soil and reinforcement on excess porewater pressure generation during undrained loadings.

The modified porewater pressure parameter B^* is defined as

$$B^* = \frac{\Delta u_r}{\sigma_{3add}} \tag{10}$$

where Δu_r is the porewater pressure difference between the unreinforced and reinforced specimens. Specifically, the parameter B^* reflects the influence of reinforcement on the enhanced additional confining pressure and porewater pressure difference. The B^* value is typically less than 1.0 (*i.e.*, $\sigma_{3add} > \Delta u_r$) for permeable reinforcement and a smaller B^* value indicates the higher effective additional confining pressure σ'_{3add} developed inside the specimens, resulting in higher shear strength improvement of the reinforced clay.

The modified porewater pressure parameter A^* is expressed as

$$A^* = \frac{u - \Delta u_r}{\sigma_d - \sigma_{3add}} \tag{11}$$

where u is the excess porewater pressure of the reinforced clay at failure. The modified porewater pressure parameter A^* is similar to that defined in Ingold and Miller's method with B' replaced by B^* in Eq. (8) to avoid assuming the B' value ($B' = 1.0$ assumed in Ingold and Miller's method). The effect of reinforcement was intentionally removed by subtracting Δu_r and σ_{3add} in the numerator and denominator of Eq. (11); the modified porewater pressure parameter A^* can solely reflect the effect of soil on porewater pressure generation. Therefore, the influence of the soil and reinforcement can be separated using the proposed parameters A^* and B^*.

4.3 Comparison of Porewater Pressure Parameters

Table 5 summarizes the porewater pressure parameter values calculated through different methods. In Skempton's method, A values for unreinforced specimens vary from –0.13 to 0.23 for $\sigma'_{3,con}$ in the range 50 ~ 200 kPa. This variation in A values for the unreinforced soil is associated with the overconsolidation ratio, as discussed in Section 3.1. For the reinforced specimen, the calculated A value at a given $\sigma'_{3,con}$ increases as the number of reinforcement layers increases. The observed increasing trend may create a misunderstanding that the influence of reinforcement on porewater pressure generation is more marked than that on soil shear strength improvement. This confusion is because the effect of additional confining pressure induced by reinforcement is not considered in Skempton's porewater pressure parameter A as it was originally developed for unreinforced soil. Therefore, it is inappropriate to interpret the porewater pressure generation of reinforced specimens using Skempton's method.

In Ingold and Miller's method, the value of porewater pressure A' decreases as the number of reinforcement layers increases. These analytical results agree with the A' trend reported by Ingold and Miller (1982) for the tests on clay reinforced through porous plastic during CU tests. However, as discussed previously, the effects of soil and reinforcement on excess porewater pressure generation are not separated appropriately in Ingold and Miller's method; therefore, it becomes difficult to assess the sole effect of reinforcement on porewater pressure generation and its relationship with shear strength improvement. As shown in Table 5, the A' values vary not only with different reinforcement layers but also with different $\sigma'_{3,con}$, suggesting that both soil and reinforcement can affect the A' value.

Table 5 and Fig. 14 list the results of the modified porewater pressure parameters A^* and B^* estimated through the proposed method. A^* depends on the soil stress history (*i.e.*, $\sigma'_{3,con}$ value) and not on the reinforcement layers. As shown in Fig. 14, only a small variation in A^* is observed when increasing the number of reinforcement layers (or reducing the reinforcement spacing), demonstrating that the modified parameter A^* can exclude the effect of reinforcement and solely reflect the effect of soil on porewater pressure generation.

The values of the modified porewater pressure parameter B^* range from 0.4 to 0.9 and decrease consistently with increase in reinforcement layers, regardless of $\sigma'_{3,con}$ (Fig. 14(b)). The lower B^* value indicates that the reinforcement is more effective in enhancing σ_{3add} than increasing Δu_r (*i.e.*, $\sigma_{3add} > \Delta u_r$); therefore, a higher effective additional confining pressure is developed inside the specimens, resulting in higher shear strength improvement of the reinforced clay. This statement is supported by the result that the soil shear strength increases as the number of reinforcement layers increases. The data in Table 5 and Fig. 14(b) prove that the B^* can be used to effectively quantify the effect of reinforcement on porewater pressure generation and its relationship with soil shear strength improvement.

Table 5 Comparison of porewater pressure parameters by different methods

Cases	σ_d (kPa)	u (kPa)	Δu_r (kPa)	σ_{3add} (kPa)	Skempton's method	Ingold and Miller's method	Proposed method	
					A	A'	A^*	B^*
$\sigma'_{3,con}$ = 50 kPa								
Unreinforced	188.5	–24.4	0	0	–0.13	–0.13	–0.13	*N/A*
1 layer	207.3	–15.8	8.6	12.1	–0.08	–0.14	–0.13	0.71
2 layers	243.8	–6.7	17.7	30.6	–0.03	–0.18	–0.11	0.58
3 layers	327.1	2.5	26.9	65.3	0.01	–0.24	–0.10	0.41
$\sigma'_{3,con}$ = 100 kPa								
Unreinforced	220	–6	0	0	–0.03	–0.03	–0.03	*N/A*
1 layer	256.6	19.6	25.6	29.4	0.08	–0.04	–0.03	0.87
2 layers	283.8	32.1	38.1	46.9	0.11	–0.06	–0.03	0.81
3 layers	330	52.8	58.8	76.4	0.16	–0.09	–0.02	0.77
$\sigma'_{3,con}$ = 200 kPa								
Unreinforced	295	68.2	0	0	0.23	0.23	0.23	*N/A*
1 layer	314.7	81.0	12.8	15.2	0.26	0.22	0.23	0.84
2 layers	373.4	102.5	34.3	49.5	0.27	0.16	0.21	0.70
3 layers	410.1	118.7	50.5	72.7	0.29	0.14	0.20	0.69

Note: All the porewater pressure parameters are evaluated at soil limit state (ε_1 = 15%). N/A indicates "Not Applicable"

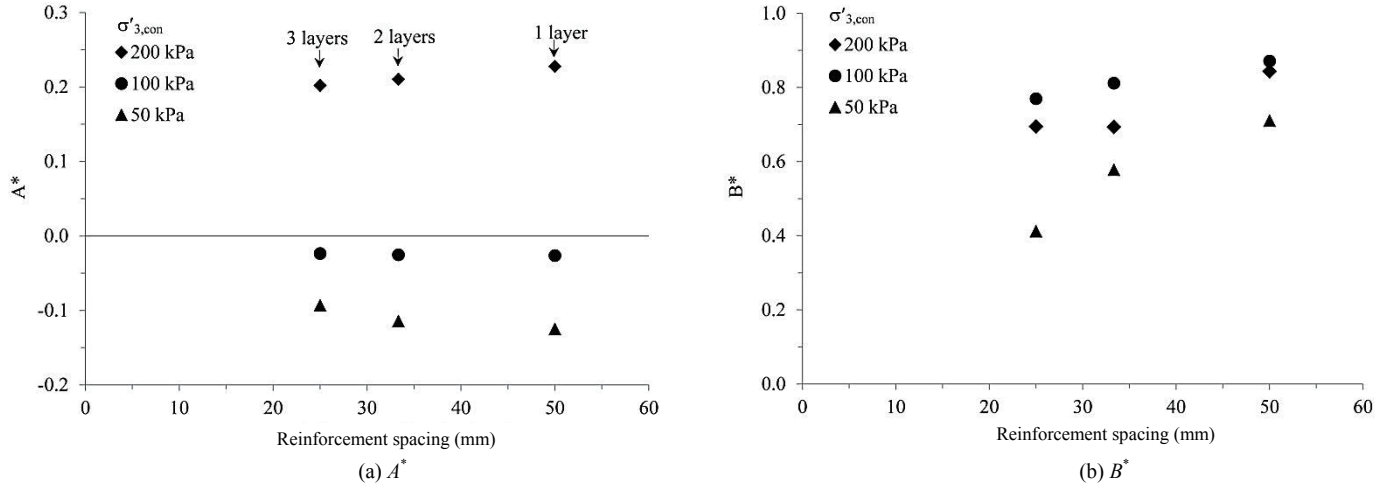

Fig. 14 Modified porewater pressure parameters A^* and B^* at ε_1 = 15% for reinforced clay: (a) A^*; (b) B^*

5. CONCLUSIONS

A series of CU triaxial compression tests were performed to investigate the shear behavior and porewater pressure generation of the reinforced clay specimens with various nonwoven geotextile layers. The main objective of this study was to investigate the generation of excess porewater pressure for reinforced clay and its relation with the shear strength improvement of reinforced clay. A modified porewater pressure parameter was proposed to assess the effect of reinforcement on excess porewater pressure generation during undrained loadings. The conclusions of this study are summarized as follows:

- Nonwoven geotextile as a permeable reinforcement reduced the required time for consolidation but its high compressibility induced higher volume reduction compared with unreinforced clay.
- The shear strength of the reinforced clay and porewater pressure at failure increased as the number of reinforcement layers increased because of the lateral restraint of the reinforced clay from the mobilized tensile force of reinforcement layers.
- Both effective and total stress failure envelopes of the reinforced clay shifted upward as the number of reinforcement

layers increased and appeared to be parallel to those of the unreinforced clay. The difference in the friction angle was minor.

- On the basis of the additional confinement approach, modified porewater pressure parameters, A^* and B^*, for the reinforced clay were proposed to quantitatively assess the influence of soil and reinforcement on the excess porewater pressure generation, respectively, during undrained loadings. The A^* value is close to Skempton's porewater pressure parameter A for unreinforced soil. The B^* is defined as the ratio of porewater pressure difference to additional confining pressure. The lower B^* value indicates that the reinforcement is more effective in enhancing additional confining pressure than increasing excess porewater pressure.
- This study demonstrated that the effect of geotextile layers on inducing additional confinement was more marked than that on the development of porewater pressure, resulting in an increase in effective confining pressure and subsequently in the shear strength improvement of reinforced clay.

Finally, it should be reminded that the data presented in this study relates to laboratory tests on saturated clay reinforced with flexible nonwoven geotextile under triaxial undrained conditions. The conducted tests were intended to simulate the worst conditions of reinforced soil, although these conditions deviate considerably from those likely to prevail on site, where the soil is most likely partially saturated. In addition, the reinforcement with higher stiffness and tensile strength is typically used for the GRS structures in the field. Despite these differences, the test data are expected to provide useful and insightful information to understand the behavior and failure mechanism of reinforced earth.

ACKNOWLEDGEMENTS

The financial support for this research was from the Ministry of Science and Technology of Taiwan under grant no. NSC102-2221-E-011-057-MY3. The financial supports for the second and third authors during their graduate study were provided by the Taiwan Ministry of Education under the grant for "Aim for the Top-Tier University Project". These financial supports are gratefully acknowledged.

REFERENCES

AASHTO, (2002). *Standard Specifications for Highway Bridges*. 17th edition, American Association of State Highway and Transportation Officials, Washington, D.C.

ASTM D422, *Standard Test Method for Particle-Size Analysis of Soils*. ASTM International, West Conshohocken, PA, USA.

ASTM D4491, *Standard Test Methods for Water Permeability of Geotextiles by Permittivity*. ASTM International, West Conshohocken, PA, USA.

ASTM D4595, *Standard Test Method for Tensile Properties of Geotextiles by the Wide-Width Strip Method*. ASTM International. West Conshohocken, PA, USA.

ASTM D4767, *Standard Test Method for Consolidated Undrained Triaxial Compression Test for Cohesive Soils*. ASTM International, West Conshohocken, PA, USA.

Al-Omari, R.R., Al-Dobaissi, H.H., Nazhat, Y.N., and Al-Wadood, B.A. (1989). "Shear strength of geomesh reinforced clay." *Geotextiles and Geomembranes*, **8**(4), 325–336.

Athanasopoulos, G.A. (1993). "Effect of particle size on the mechanical behaviour of sand-geotextile composites." *Geotextile and Geomembranes*, **12**(3), 255–273.

Bathurst, R.J. and Karpurapu, R. (1993). "Large-scale triaxial compression testing of geocell reinforced granular soils." *Geotechnical Testing Journal*, ASTM, **16**(3), 293–303.

Bathurst, R.J., Vlachopoulos, N., Walters, D.L., Burgess, P.G., and Allen, T.M. (2006). "The influence of facing stiffness on the performance of two geosynthetic reinforced soil retaining walls." *Canadian Geotechnical Journal*, **43**(12), 1225–1237.

Berg, R., Christopher, B.R., and Samtani, N. (2009). *Design of Mechanically Stabilized Earth Walls and Reinforced Soil Slopes*. Vol. I and II, Report No. FHWA-NHI-10-024, National Highway Institute, Federal Highway Administration, Washington, D.C.

Casagrande, A. (1936). "The determination of the preconsolidation load and its practical significance." *Proceedings of the 1st International Conference, Soil Mechanics and Foundation Engineering*, 60.

Chandrasekaran, B., Broms, B.B., and Wong, K.S. (1989). "Strength of fabric reinforced sand under axisymmetric loading." *Geotextiles and Geomembranes*, **8**(4), 293–310.

Chen, J. and Yu, S. (2011). "Centrifugal and numerical modeling of a reinforced lime-stabilized soil embankment on soft clay with wick drains." *International Journal of Geomechanics*, **11**(3), 167–173.

Christopher, B.R. and Stuglis, R.S. (2005). "Low permeable backfill soils in geosynthetics reinforced soil wall: State of the practice in North America: State of the practice in North America." *Proceedings of North American Geo-synthetics Conference*, Las Vegas, Nevada, USA

Elias, V., Christopher, B.R., and Berg, R. (2001). *Mechanically Stabilized Earth Walls and Reinforced Soil Slopes Design and Construction Guidelines*. Report No. FHWA-NHI-00-043, National Highway Institute, Federal Highway Administration, Washington, D.C.

Fabian, K. and Foure, A. (1986). "Performance of geotextile-reinforced clay samples in undrained triaxial tests." *Geotextiles and Geomembranes*, **4**(1), 53–63.

Fourie, A.B. and Fabian, K.J. (1987). "Laboratory determination of clay geotextile interaction." *Geotextiles and Geomembranes*, **6**(4), 275–294.

Glendinning, S., Jones, C., and Pugh, R. (2005). "Reinforced soil using cohesive fill and electrokinetic geosynthetics." *International Journal of Geomechanics*, **5**(2), 138–146.

Gray, D.H. and Al-Refeai, T. (1986). "Behavior of fabric vs. fiber reinforced sand." *Journal of Geotechnical Engineering*, ASCE, **112**(8), 804–820.

Haeri, S.M., Noorzad, R., and Oskoorouchi, A.M. (2000). "Effect of geotextile reinforcement on the mechanical behavior of sand." *Geotextiles and Geomembranes*, **18**(6), 385–402.

Hausmann, M.R. (1976). "Strength of reinforced soil." *Proceedings of the 8th Australasian Road Research Conference*, Perth, Australia, **8**(13), 1–8.

Indraratna, B., Satkunaseelan, K.S., and Rasul, M.G. (1991). "Laboratory properties of a soft marine clay reinforced with woven and nonwoven geotextiles." *Geotechnical Testing Journal*, ASTM, **14**(3), 288–295.

Ingold, T.S. (1983). "Reinforced clay subject to undrained traxial loading." *Journal of Geotechnical Engineering*, ASCE, **109**(5), 738–744.

Ingold, T.S. and Miller, K.S. (1982). "The performance of impermeable and permeable reinforcement in clay subject to undrained loading." *Quarterly Journal of Engineering Geology and Hydrogeology*, **15**(3), 201–208.

Ingold, T.S. and Miller, K.S. (1983). "Drained axisymmetric loading of reinforced clay." *Journal of Geotechnical Engineering*, ASCE, **109**(7), 883–898.

Jamei, M., Villard, P., and Guiras, H. (2013). "Shear failure criterion based on experimental and modeling results for fiber-reinforced clay." *International Journal of Geomechanics*, **13**(6), 882–893.

Khedkar, M.S. and Mandal, J.N. (2009). "Behaviour of cellular reinforced sand under triaxial loading conditions." *Geotechnical and Geological Engineering*, **27**(5), 645–658.

Mirzababaei, M., Miraftab, M., Mohamed, M., and McMahon, P. (2013). "Unconfined compression strength of reinforced clays with carpet waste fibers." *Journal of Geotechnical and Geoenvironmental Engineering*, ASCE, **139**(3), 483–493.

Mitchell, J.K. and Zomberg, J.G. (1995). "Reinforced soil structures with poorly draining backfills. Part II: Case histories and applications." *Geosynthetics International*, **2**(1), 265–307.

Nguyen, M.D., Yang, K.H., Lee, S.H., Wu, C.S., and Tsai, M.H. (2013). "Behavior of nonwoven geotextile-reinforced soil and mobilization of reinforcement strain under triaxial compression." *Geosynthetics International*, **20**(3), 207–225.

Noorzad, R. and Mirmoradi, S.H. (2010). "Laboratory evaluation of the behavior of a geotextile reinforced clay." *Geotextiles and Geomembranes*, **28**(4), 386–392.

Raisinghani, D.V. and Viswanadham, B.V.S. (2011). "Centrifuge model study on low permeable slope reinforced by hybrid geosynthetics." *Geotextiles and Geomembranes*, **29**(1), 567–580.

Schlosser, F. and Long, N.T. (1974). "Recent results in French research on reinforced earth." *Journal of the Construction Division*, ASCE, **100**(3), 223–237.

Skempton, A.W. (1954). "The pore-pressure coefficient A and B." *Gétechnique*, **4**(4), 143–147.

Sridharan, A., Murthy, S., Bindumadhava, B.R., and Revansiddappa, K. (1991). "Technique for using fine-grained soil in reinforced earth." *Journal of Geotechnical Engineering*, ASCE, **117**(8), 1174–1190.

Taechakumthorn, C. and Rowe, R. (2012). "Performance of reinforced embankments on rate-sensitive soils under working conditions considering effect of reinforcement viscosity." *International Journal of Geomechanics*, **12**(4), 381–390.

Unnikrishnan, N., Rajagopal, K., and Krishnaswamy, N.R. (2002). "Behaviour of reinforced clay under monotonic and cyclic loading." *Geotextiles and Geomembranes*, **20**(2), 117–133.

Wu, C.S. and Hong, Y.S. (2008). "The behavior of a laminated reinforced granular column." *Geotextiles and Geomembranes*, **26**(4), 302–316.

Yang, K.H., Yalew, W.M., and Nguyen, M.D. (2015). "Behavior of geotextile-reinforced clay with a coarse material sandwich technique under unconsolidated-undrained triaxial compression." *International Journal of Geomechanics*, ASCE, DOI: 10.1061/(ASCE) GM.1943-5622.0000611.

Zornberg, J.G. and Mitchell, J.K. (1994). "Reinforced soil structures with poorly draining backfills. Part I: Reinforcement interactions and functions." *Geosynthetics International*, **1**(2), 103–148.